International Journal of Technology

http://ijtech.eng.ui.ac.id

Research Article

Kaolinite-Based Photocatalysts for Azo Dyes Degradation under Xenon and Sunlight Irradiations: The Effects of Electro-Deionization and Impregnation Methods

Khoirina Dwi Nugrahaningtyas [1,*], IF Nurcahyo[1], Desinta Yulyana Putri [1], Sri Juari Santoso[2], Eny Kusrini [3,4,5,], Anwar Usman[6], Lee D. Wilson[7]**

[1] *Department of Chemistry, Faculty of Mathematics and Natural Sciences, Sebelas Maret University, Jl. Ir Sutami No 36A, Surakarta, 57126, Indonesia*
[2]*Department of Chemistry, Faculty of Mathematics and Natural Sciences, Universitas Gadjah Mada, Sekip Utara PO BOX BLS 21 Yogyakarta 55281, Indonesia*
[3]*Department of Chemical Engineering, Faculty of Engineering, Universitas Indonesia, Kampus Baru UI, Depok 16424, Indonesia*
[4]*Research Group of Green Product and Fine Chemical Engineering, Laboratory of Chemical Product Engineering, Department of Chemical Engineering, Universitas Indonesia, Kampus Baru UI, Depok, 16424, Indonesia*
[5]*Tropical Renewable Energy Research Center, Faculty of Engineering, Universitas Indonesia, Kampus Baru UI, Depok, 16424, Indonesia*
[6]*Department of Chemistry, Faculty of Science, Universiti Brunei Darussalam, Jalan Tungku Link, Gadong, Brunei Muara, BE1410, Brunei Darussalam*
[7]*Department of Chemistry, University of Saskatchewan 110 Science Place, Room 156 Thorvaldson Building, Saskatoon, SK S7N 5C9, Canada*

**Corresponding author: khoirinadwi@staff.uns.ac.id; Tel.: +62-*
*** Corresponding author: eny.k@ui.ac.id; Tel.: +62-7863516 ext 204*

Abstract: Azo dyes pose a significant environmental concern due to their high stability and resistance to natural degradation. To address this issue, we explored kaolinite-based photocatalysts for azo dye degradation with a methylene blue (MB) as an azo dye model. In the present study, the transition metals-kaolinite composites (TMs-kaolinite) where TM = Fe, Ni, or Zn) were prepared by two methods, namely electro-deionization (ED) and impregnation (IMP) methods. The performance of TMs-kaolinite photocatalysts for azo dye degradation were evaluated using the xenon and sunlight irradiations. The activities of the degradation reaction of MB were observed by varying photocatalyst types, time illumination and type irradiation. We found that the most excellent photocatalytic activity for degradation of MB is the Zn-Kaolinite IMP with efficiency 92% during 90 minutes of irradiation. Meanwhile, the pristine kaolinite is only showing the best adsorbent for removal of MB without degradation process with adsorption efficiency of 98%. Overall, the results indicated that the TMs-kaolinite showed high photocatalytic activity for degradation of azo dye, with the sunlight irradiation is more effective than the xenon irradiation. Different forms of TMs-kaolinite catalysts have also different phenomena and mechanisms for photodegradation of MB. We found that the TMs in TMs-kaolinite have important role in the performance of photocatalysts.

This work was supported by the Universitas Sebelas Maret and funded by the Indonesian Collaboration Research Program (RKI) Scheme C [Decision Letter No. 767/UN27/HK/2023 and Contract No. 590.1/UN27.22/HK.07.00/2023.

https://doi.org/xx/ijtech.xx
Received date; Revised date; Accepted date

Keywords: Azo dyes; Electro-Deionization and Impregnation; Kaolinite; Photodegradation; Sunlight; Transition metals.

1. Introduction

Rapid industrialization has increased pollution associated with wastewater discharge and exhaust emissions. These environmental contaminants can threaten human health and long-term development (Mousavi, Habibi-Yangjeh and Abitorabi, 2016; Wang, Jiang and Gao, 2022). One of the fastest-growing industries is the textile industry and its derivatives. Economic reasons and the lack of knowledge of business actors prevent waste processing from being carried out properly and tend to be haphazard.

Azo dyes are widely utilized in the textile, leather, cosmetic, food, and paper sectors (Sudha and Saranya, 2014). Azo dyes, when dumped into aquatic habitats, mix with water, collect, and enter the bodies of aquatic biota, resulting in bioaccumulation. Physically, azo dyes that enter the river make the river water colored and block light from entering the water body, thus affecting the photosynthesis process of phytoplankton or aquatic plants, which will also affect zooplankton and other aquatic organisms. Chemically, it can reduce oxygen levels in polluted waters and result in the death of aquatic biota. Simultaneously, azo dyes that degrade anaerobically in aquatic environments can yield aromatic amine compounds far more hazardous than the azo dye itself due to their high toxicity. One example of a compound formed in the anaerobic process is chloroaniline, which can harm human health because it is thought to affect respiratory organs, urogenital organs, and nervous disorders(Santos, Dos Santos and Andrade, 2021). The complex aromatic structure of the azo dye makes it difficult to degrade by traditional biological processing processes (Wang, Jiang and Gao, 2022). Therefore, we need an effective processing method to degrade the dye.

Dye degradation usually utilizes photon energy, such as UV radiation or sunshine. Sunlight has a higher intensity and longer wavelength (310–2300 nm) than UV light (200–380 nm). Furthermore, sunlight is a combination of approximately 45% visible light and approximately 3% UV light. So, sunlight has relatively high energy and can provide a large amount of photon energy, indicating that using sunlight irradiation will improve the degradation process.

Recently, photocatalysis techniques have been developed for environmental remediation due to their low cost, environmental friendliness, nontoxicity, and stability (Zyoud *et al.*, 2019). One porous material widely used as a photocatalyst for dye waste processing is kaolinite. Kaolinite is known for its layered and porous structure, which offers several advantages. It is non-corrosive, inexpensive, environmentally friendly, and abundant. The high surface area and the abundance of hydroxyl (OH) groups on Kaolin's surface contribute to its photocatalytic capabilities (Cao, Wang and Cheng, 2021).

However, previous studies have found that kaolinite modified with metal can increase the efficiency of kaolinite photodegradation (Chen *et al.*, 2023; da Trindade *et al.*, 2024). Increasing photocatalytic efficiency can be done by designing the structure, doping metals or non-metals, heterojunctions, and surface modifications (Li *et al.*, 2020; Cao, Wang and Cheng, 2021). One method to increase the photocatalytic efficiency of clay is by converting it into a composite based on a combination of clay and semiconductors (Janíková *et al.*, 2017; Wongso *et al.*, 2019; Zyoud *et al.*, 2019). This performs because the semiconductors expand the clay absorption range of visible light waves, thereby increasing the degradation rate of environmental organic pollutants. Previous research showed that Fe was more effective in upgrading the efficiency of clay in the photodegradation process for dye than Mn (Balarabe *et al.*, 2022). Meanwhile, although Co metal is effective in photocatalytic applications, this metal is more expensive than Ni, Zn, and Fe metals (Türkyılmaz, Güy and Özacar, 2017). These transition metals in the form of oxides have low band gaps, especially in Fe metal oxide (Fe_2O_3) of 2.2 eV, while Ni metal oxides (NiO) and Zn (ZnO) have band gaps of 3.6-4 eV and 3.37 eV, respectively (Da Trindade *et al.*, 2019; Seo *et al.*, 2019).

Several methods, such as impregnation (Asmare *et al.*, 2022), sol-gel (Shao *et al.*, 2015), precipitation (Wongso *et al.*, 2019), hydrothermal (Mamulová Kutláková, Tokarský and Peikertová, 2015), and ion exchange (Hakimi, Ghorbanpour and Feizi, 2018) have been reported to synthesize metal@kaolinite composites. Among these methods, most are relatively complicated because their preparation involves many steps, is less efficient, and requires high energy, except impregnation, which is a simpler method. The impregnation process involves modifying a support material by

filling its pores with an active metal solution via immersing the support in a solution that contains the active metal (Nugrahaningtyas *et al.*, 2022; Heriyanto *et al.*, 2023; Aviantara *et al.*, 2024). Meanwhile, a new method, namely electro-deionization, has been proposed to enhance this synthesis of metal@kaolites composites. This method combines the ion exchange method with an electrolysis system. This new method is efficient because it is simple, easy to prepare with safe precursors, and optimal for replacing balancing cations. The principle of the new method is based on the exchange of ion metals by utilizing the difference in electrical potential in the transport of metal ions (Pal, Dixit and Lal, 2016; Li *et al.*, 2019).

Therefore, the aim of the study is to compare the impregnation and ED methods on the character of the transition metals-kaolinite composites (TMs-kaolinite) catalysts. Methylene blue (MB) is selected a model azo dye, was used to test the periodicity of transition metals Fe, Ni, and Zn combined with kaolinite. Previous research shows a relationship between the periodic properties of elements and their catalytic properties (Nugrahaningtyas *et al.*, 2022, 2025). The other research found that photocatalytic degradation of MB using TiO_2 has been reported by Suhaimi et al. (2022), and Zulmajdi et al. (2019), kaolin-titania (Kamaluddin et al., 2021) and samarium complexes with 2,6-Naphtalenedicarboxylate ligand (Wulandari et al., 2019). Different forms of composites have different phenomena and mechanisms for the photodegradation of MB. Thus, this study is important to evaluate the different methods and the effect of TMs in forming of (TMs-kaolinite) catalysts. Various material engineering has been and continues to be carried out to obtain the best physical, chemical, and biological properties for future material use, especially as a photocatalyst material. A UV-Vis was employed to quantify the precise concentration of the MB solution post-degradation.

2. Methods

2.1. Materials and Instruments

The $Ni(NO_3)_2$, $Zn(NO_3)_2$, or $Fe(NO_3)_3$ salts with a pro-analysis grade were purchased from Merck (Germany). The metal electrodes and electro-deionization tool kit were purchased from Edulab. The instruments used to characterize catalyst samples are Scanning Electron Microscope (SEM) (JEOL JSM 6510 LA) equipped with EDAX APEX, X-ray fluorescence spectrometry (Ranger BRUKER S2 puma), X-ray diffractometer (Shimadzu 7000) with Cu-Ka radiation (k = 1.540 Å), infrared spectrophotometer (FTIR Spectrophotometer, Shimadzu 8201 PC), and gas sorption analyzer (Quantachrome St. 3 on Nova Touch 4LX). Analysis of dye concentration was carried out using UV Vis (Double Beam Spectrophotometer HITACHI UH5300).

2.2.Preparation of TMs@kaolinite by Electro-Deionization Method

The salt bridge from kaolinite is made into pellets by pressing with filter paper on both sides, 3 cm long and 22.5 cm in diameter. The salt bridge is placed in an ED circuit device. Then, the two pure metal electrodes (Ni, Zn, or Fe) are placed alternately in each container on the device. The electrodes were made with a length of 7.5 cm and a width of 1.6 cm. Then, the ED circuit is inserted into the $Ni(NO_3)_2$, $Zn(NO_3)_2$, or $Fe(NO_3)_3$ solutions alternately. The electrolyte solution was made to a concentration of 0.1 M. The electro-ion exchange process used a voltage of 28.4 V and a current of 0.01 A for 3 hours. After the process is complete, wash with sufficient demineralization water. TMs@kaolinite is oven at 110 °C for 3 hours, then calcination with air at 500 °C for 3 hours. The catalyst obtained is called TMs@kaolinite ED. The samples were characterized using XRD, FTIR, XRF, SEM, and SAA to determine the metals' nature, character, and content.

2.3. Preparation of TMs@kaolinite Impregnation Method (IMP)

The impregnation method of catalyst preparation follows a modified version of an earlier procedure (Asmare *et al.*, 2022; Nugrahaningtyas *et al.*, 2022). One hundred milliliters of demineralization water were used to make a suspension of the kaolinite, stirring at room temperature for 30 minutes at 900 rpm. The suspension was filtered and mixed with an electrolyte solution (Ni $(NO_3)_2$, Zn $(NO_3)_2$, or Fe $(NO_3)_3$) made to a concentration of 0.1 M. The impregnation process was carried out in two stages. The first stage of the impregnation process lasts 16 hours at 30°C. The second stage was an impregnation process for 4 hours at 80°C. After impregnation, the catalyst is dried and calcined for 3 hours at 500°C. XRD, FTIR, XRF, SEM, and SAA were used to evaluate the type, character, and content of metal ions in TMs@kaolinite.

2.4. Characterizations

The morphology and size of the monoliths were studied with scanning electron microscopy (SEM). The elemental composition was analyzed using X-ray fluorescence spectrometry. An X-ray diffractometer (Shimadzu 7000) was used for diffraction pattern and phase composition analysis. The functional groups of the photocatalyst were detected using an infrared spectrophotometer (FTIR Spectrophotometer, Shimadzu 8201 PC). The catalyst's pore size and BET surface area were obtained from a gas sorption analyzer (Quantachrome St. 3 on Nova Touch 4LX). Analysis of dye concentration before and after testing was carried out using a UV Vis.

2.5. Photocatalytic Activity Test of Azo Dyes

The previous method was adjusted to measure the samples' photocatalytic activity (Setiadi et al. 2023). Methylene Blue, which was chosen as a model of Azo dye, was dissolved in demineralization water until a solution of 1000 ppm was obtained. Take enough and dilute to 20 ppm. A photocatalytic test was performed on TMs@kaolinite without light, with artificial irradiation, and with natural sunlight.

The photocatalytic test without light (dark) was investigated by adding 0.1 g of TMs@kaolinite into 100 mL of 20 ppm MB and stirring at 600 rpm for 90 minutes. After 30 minutes, every 10 minutes, the solution was carefully taken using a syringe equipped with a filter (0.22 μm) and analyzed for absorbance using UV-Vis as the concentration of MB remaining in the solution. The concentration of MB was calculated using a standard curve. Then, the adsorption efficiency was calculated using equation 1.

$$Adsorption\ efficieny = \frac{[MB]_{initial} - [MB]_{final}}{[MB]_{initial}}\ x\ 100\% \quad (1)$$

where *[MB]* is the concentration of Methylene blue.

A similar procedure was used to perform the photocatalytic test under a xenon lamp (Michiba H1 Xenon white 5000k Bohlam Mobil Halogen 55 W – 12 V) as an artificial lighting resource. First, to homogenize the suspension, 0.1 g of TMs@kaolinite was added to 100 mL of 20 ppm MB and stirred at 600 rpm for 30 minutes in the dark. After that, the photodegradation test was continued by artificially irradiating a xenon lamp for 1 hour, stirring at 600 rpm. Every 10 minutes, the solution was carefully taken using a syringe equipped with a filter (0.22 μm), and its absorbance was analyzed using UV-Vis.

2.6.The adsorption kinetic modeling

To calculate the kinetics of MB removal in this study, pseudo-first-order (PFO), and pseudo-second-order (PSO) kinetic models were used (Darmadi *et al.*, 2023; Tsaviv *et al.*, 2024). Based on the linear regression form of PFO and PSO, the reaction order is determined based on the correlation value (R2).

3. Results and Discussion

3.1. SEM studies

The structure of pristine kaolinite shows a flat plate-like shape that is stacked and arranged in layers and regularly (see Figure 1a). These layers are connected through hydrogen bonds, contributing to kaolinite's unique structure and characteristics (Ivanić *et al.*, 2015). Through chemical or physical modification, the surface and pores can be altered better to support the placement and reaction of the photocatalyst particles. This modification can improve the interaction between the photocatalyst and the substrate, increasing the efficiency of the photochemical reaction. Although kaolinite is not a natural semiconductor, this modification allows kaolinite to act as an effective media support in photocatalytic reactions.

Adding metal to kaolinite causes the distance between the layers to widen, which indicates that the metal has succeeded in inserting itself between the kaolinite layers. The TMs@kaolinite showed damage in several parts, decreased regularity, and widening of the interlayer distance compared to kaolinite (See Figure 1b-1g). This phenomenon, due to Ni, Zn, and Fe metal particles, can disrupt hydrogen bonds between layers, causing changes in the structure of kaolinite. The larger size of the metal particles compared to the interlayer space of kaolinite causes binding to the kaolinite surface penetrating the interlayer space, damaging the kaolinite sheet. These structural changes can increase

particle reactivity because larger particles have a higher surface area and more active reaction sites (Yahaya *et al.*, 2017; Ramadji *et al.*, 2022).

There are differences in structural changes between the ED and IMP methods. In the IMP method, the layers are still clearly visible because only metal insertion widens the distance between layers. In contrast, in the ED method, there is a change of ions that greatly changes the crystal structure. The layer structure of the TMs@kaolinite ED appears damaged due to overlapping or collapse between kaolinite layers. In addition, it is also possible that there is coagulation in the pores of the kaolinite layer, which can occur during a less-than-optimal calcination process. These structural characteristics not only increase the specific surface area but also increase the porosity ratio. Therefore, both methods significantly improve the surface properties of pristine kaolinite, which cause partial irregularities in particle shape and reduce crystal regularity on the kaolinite surface.

After impregnation, the clay morphology demonstrates that the layers are uneven and irregular due to TMs's coating of the kaolinite surface (See Figure 1e-1g). The EDX data confirms the results of investigations, which detect the presence of SiO_2, Al_2O_3, and the metals Ni, Zn, and Fe. The Fe/kaolinite IMP has the greatest metal content at 5.71% loading. This data suggests that the IMP procedure successfully incorporates more Fe metal into the kaolinite.

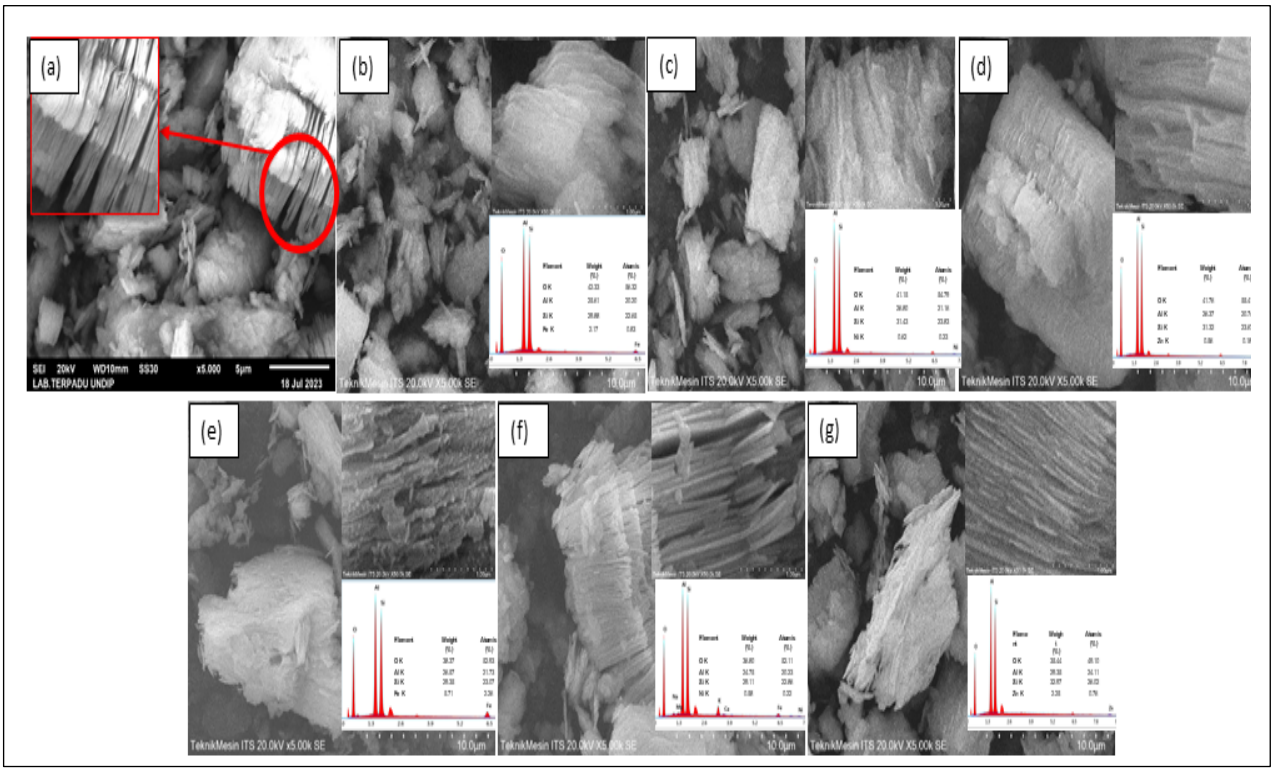

Figure 1 Morphology of (a) pristine kaolinite, (b) Fe@kaolinite ED, (c) Ni@kaolinite ED, (d) Zn@kaolinite ED, (e) Fe@kaolinite IMP, (f) Ni@kaolinite IMP, and (g) Zn@kaolinite IMP.

3.2. XRD studies

After TMs@kaolinite ED shows that most metals are successfully embedded in kaolinite. Analysis using XRD showed that the addition of metal damaged the main structure of kaolinite (Figure 2). The investigation revealed that the kaolinite employed in this investigation is the kaolinite phase having the formula $Al_2(Si_2O_5)(OH)_4$, the ICDD # 00-079-1570, with 100% purity. The diffraction pattern for TMS@kaolinite also confirmed the presence of kaolinite (ICDD # 00-002-0105) as the main phase. The peak shift at 2θ of around 25° is possible due to changes in basal spacing during metal loading between layers of kaolinite.

The results showed that the pristine kaolinite conformed to the ICDD standard pattern number 01-079-1570, with typical diffraction peaks appearing at 2θ = 12.4°, 19.8°, 21.2°, and 24.9°. The 2θ value correlated with d-spacing and Miller indexes, respectively, as follows: 7.09 Å (d_{010}); 4.44 Å (d_{020}); 4.17 Å (d_{111}); and 3.56 Å (d_{002}), which are the main typical diffraction patterns of kaolinite. In addition, the pristine kaolinite also contains quartz (SiO_2) as impurities, which are shown at 2θ = 20.5°, 26.69°, and 39.31° based on the ICDD standard #00-046-1045 (Beddiaf, Chihi and Leghrieb, 2015; Hariyanto *et al.*, 2021).

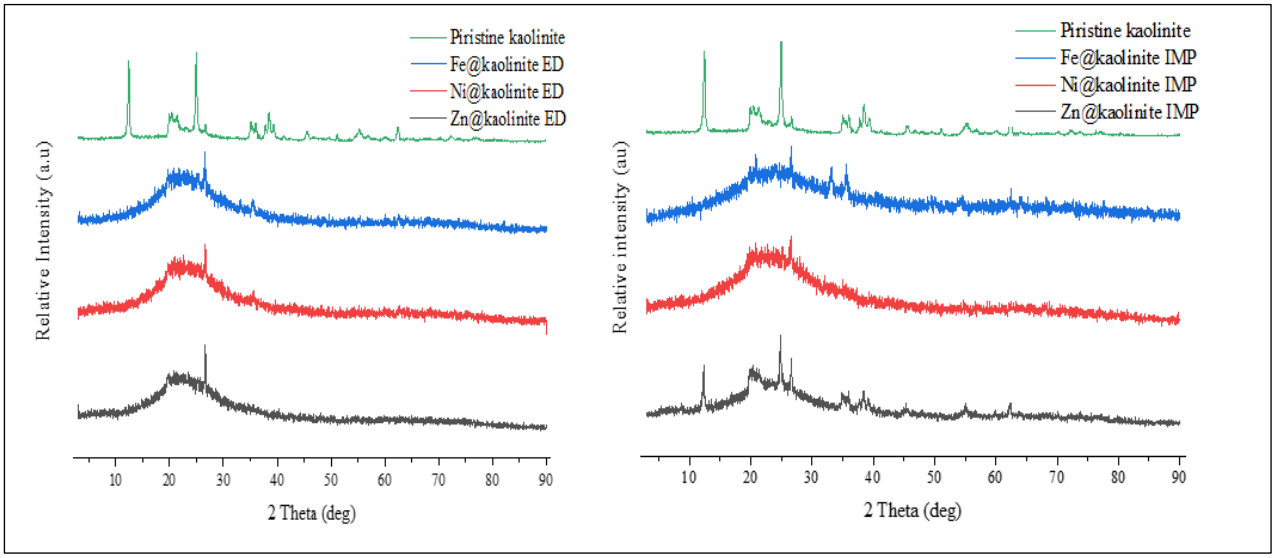

Figure 2 Comparison the XRD patterns of pristine kaolinite and TMs@kaolinite by electro-deionization (ED) and impregnation (IMP) methods.

Interpretation of the TMs@kaolinite diffraction pattern shows that adding metal causes an intensity decrease and a shift in the typical diffraction peak towards a small angle. The decrease in the intensity of the typical kaolinite diffraction peak indicates a reduction in kaolinite's crystallinity. Meanwhile, the shift in the 2θ value towards a smaller direction indicates that the distance between layers is getting wider with the presence of metal. An in-depth analysis of the TMs@kaolinite diffraction pattern shows new peaks compared to the pristine diffraction pattern.

Further analysis found that the hematite and magnetite phases were confirmed for Fe@kaolinite ED and Fe@kaolinite IMP, referring to ICDD# 00-072-0469 and 00-076-0958. The 2θ at 62.78° of Ni@kaolinite ED indicates the presence of nickel oxide (NiO) with d-spacing 1.37 Å (d_{220}) following #ICDD 00-044-1159 (Mustapha *et al.*, 2020). Unfortunately, the ED process causes some of the silica in Ni@kaolinite ED to decay and form silica dioxide (ICDD # 00-077-1060). Meanwhile, nickel is present in the dwornikite phase for Ni@kaolinite IMP, corresponding to ICDD reference #00-081-0021. Zn metal is present in both the Zn@kaolinite as zinc oxide sulfate and zinc hydroxide phases under ICDD # 00-03201475 and ICDD # 00-074-0094 (Hamrayev and Shameli, 2022).

3.3. FTIR studies

The FTIR spectra of kaolinite show the presence of four characteristic bands in the form of sharp absorptions at 3621, 3656, 3671, and 3696 cm^{-1} originating from the stretching vibration mode of the -OH function series bound to the octahedral Al atom (Al-OH) from the surface or interlayer of kaolinite (see Figure 3). The absorption bands at 3621 and 3671 cm^{-1} are caused by the inner hydroxyl (-OH) stretching region (Maged *et al.*, 2020). The Al-OH bond also appears at 3656 cm^{-1} as an octahedral structure. The Al-OH vibration caused by the alumina kaolinite sheets in coordination with the OH group is well demonstrated by the peaks at 913 and 3696 cm^{-1} (Wongso *et al.*, 2019; Wang *et al.*, 2021). The varied intensity of this band is due to the disruption of the hydroxyl through the formation of hydrogen bonds with TMs (Wang *et al.*, 2021). Both metal addition methods show that absorption at wave numbers around 3600–3750 cm^{-1} is significantly reduced after metal addition. There is a strong suspicion that ion exchange occurs between protons and metal ions. The characteristic peaks mostly disappear in the TMs@kaolinite, also indicating the destruction of the octahedral sheets of Al-OH due to the calcination treatment (Wongso *et al.*, 2019).

Meanwhile, a peak appears around 3400 cm^{-1} in TMs@kaolinite, indicating the stretching vibration of hydroxyl (Al-OH or Si-OH). The absorption around 3400 and 1639 cm^{-1} can also be attributed to the stretching and bending vibrations of H-O-H of the adsorbed water, respectively. The hydroxyl deformation of the water molecules causes a small peak at 2350 cm^{-1} in TMs@kaolinite IMP. A weak peak at 2923 cm^{-1} in TMs@kaolinite ED comes from stretching aliphatic hydrocarbons, indicating the presence of organic impurities, but their presence is insignificant due to beneficiation.

Tree peaks at around 1000 cm^{-1} correspond to the stretching vibrations of silicon monoxide (Si–O), O-Si-O, and O-Al–O-. The presence of silicon monoxide associated with the symmetric stretching vibrations of quartz, indicating that silicon oxide is predominantly in kaolinite and TMs@kaolinite. While, the appearance of O-Si-O and O-Al-O from asymmetric stretching of the aluminosilicate framework (Kusrini *et al.*, 2024). The TMs@kaolinite ED spectra showed a red shift in the asymmetric stretch of the aluminosilicate framework from 1115 cm^{-1} to 1076 cm^{-1} for Ni@kaolinite ED, Zn@kaolinite ED, and Fe@kaolinite ED. Meanwhile, the Ni@kaolinite IMP experiences a redshift to 1084 cm^{-1}, and Zn@kaolinite IMP shows a wavenumber shift to 1037 cm^{-1}. The red shift indicates that the presence of metal weakens the Si-O-S and Si-O-Al bonds. A different phenomenon occurs in Fe@kaolinite IMP, whose absorption wavenumber becomes higher (blue shift), which is 1169 cm^{-1}. According to previous research, the blue shift occurs due to the de-alumination process or releasing Al in the kaolinite structure to Al outside the framework (Holmberg, Wang and Yan, 2004). The de-alumination process causes a reduction in the amount of Al and raises the spacing of Al. The blue shift can also be due to the shortening of the Si-O-Si or Si-O-Al bonds (Nugrahaningtyas *et al.*, 2021; Zhang *et al.*, 2024).

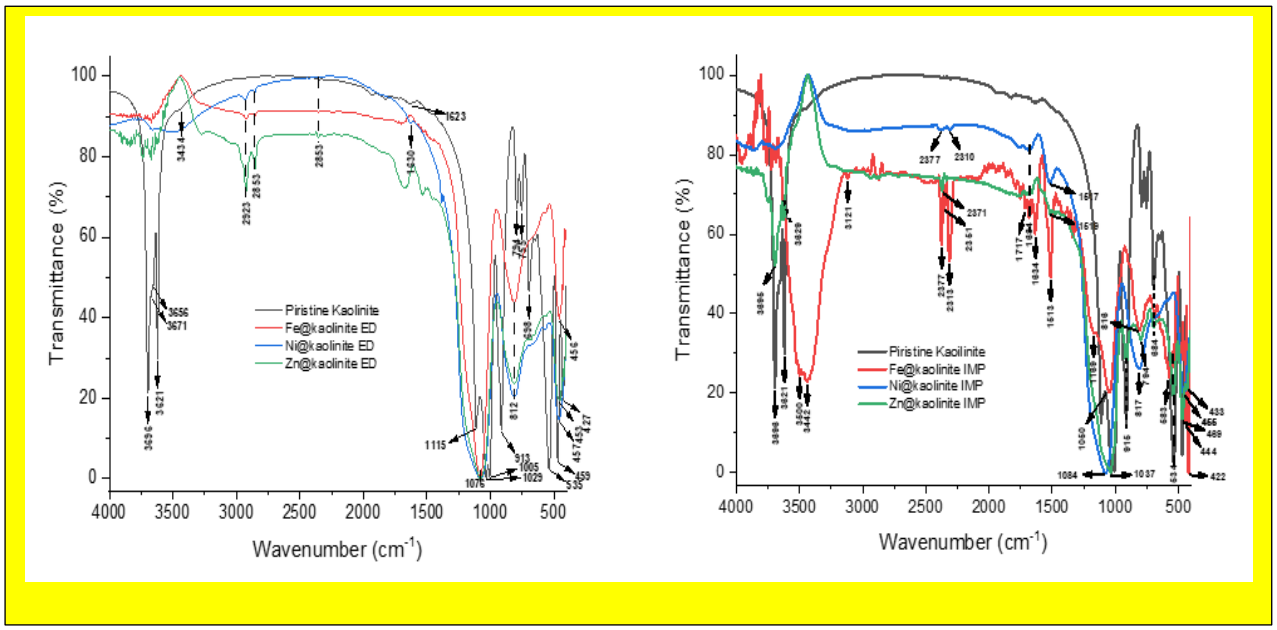

Figure 3 FTIR spectra of pristine kaolinite and TMs@kaolinite photocatalysts by electro-deionization (ED) and impregnation (IMP) methods

In the Zn@kaolinite IMP catalyst, the peak at 915 cm^{-1} is still visible, which is the Al-OH functional group in the bending mode, while in other catalysts, there is none. So, it can be concluded that adding Zn metal to kaolinite does not change the kaolinite framework. The small peak at 794 cm^{-1} is caused by metal impurities bound to aluminum and hydroxyl vibrations. The adsorption band of the M-O functional group (Al-O or Si-O) correlates with wave numbers 684, 534, and 469 cm^{-1}, indicating the presence of the Si-O functional group but in a different environment. The band at wave number 684 cm^{-1} indicates stretching vibration in Si-O. The sharp and clear peak around 534 cm^{-1} corresponds to the bending vibration of Si–O–Al, indicating that besides silica oxide, the sample also contains aluminum oxide.

The presence of metal of TMs@kaolinite ED was shown by absorption peaks at 457, 453, and 456 cm^{-1}, respectively. Meanwhile, TMs@kaolinite IMP has absorption peaks at 433, 433, and 422 cm^{-1}, respectively. The vibrations at 457 and 433 cm^{-1} indicate the presence of Ni-O from the NiO compound. The adsorption band at 453 and 433 cm^{-1} from Zn-O functional groups, and the

adsorption band at 456 and 422 cm^{-1} is from Fe-O functional groups compound due to the oxidation process of the Fe produce Fe_2O_3 compound.

The Zn@kaolinite IMP and Fe@kaolinite IMP spectra showed absorption at 534 and 583 cm-1 from a Si-O functional group bound to the Al atom (Si-O-Al). It proves that the calcination process at a temperature of 500 °C can reduce -OH with the loss of water bound to the crystal lattice and change the metal into a metal oxide that replaces the -OH group. The addition of metal by impregnation methods does not damage its main structure. So, the impregnation method is better at producing TMs@kaolinite catalysts without damaging the main structure of kaolinite; in this case, its photocatalytic properties will also increase.

3.4. Adsorption-desorption isotherm analysis

Adsorption-desorption isotherm analysis was carried out to determine the catalyst synthesis material's surface area characteristics, pore size, and pore volume (Figure 4). The BET, BJH, and t-plot methods were used to calculate the specific surface area, the pore diameter, and the pore volume. The adsorption isotherms of TMs@kaolinite and kaolinite follow the type III isotherm model of Brauneur, Deming, and Teller (BDDT). This model shows a system characterized by mesoporous dimensions and monolayer behavior. The presence of a hysteresis loop in the adsorption isotherm is typical of mesopores. Adsorption on the mesopore surface promotes the formation of multilayers, which causes capillary condensation. Therefore, the catalyst exhibits adsorption behavior similar to macropores at low pressures but is then followed by a significant increase in adsorption at higher pressures due to the capillary condensation inside the mesopores. The process of capillary condensation and evaporation at various relative pressures produces a hysteresis loop.

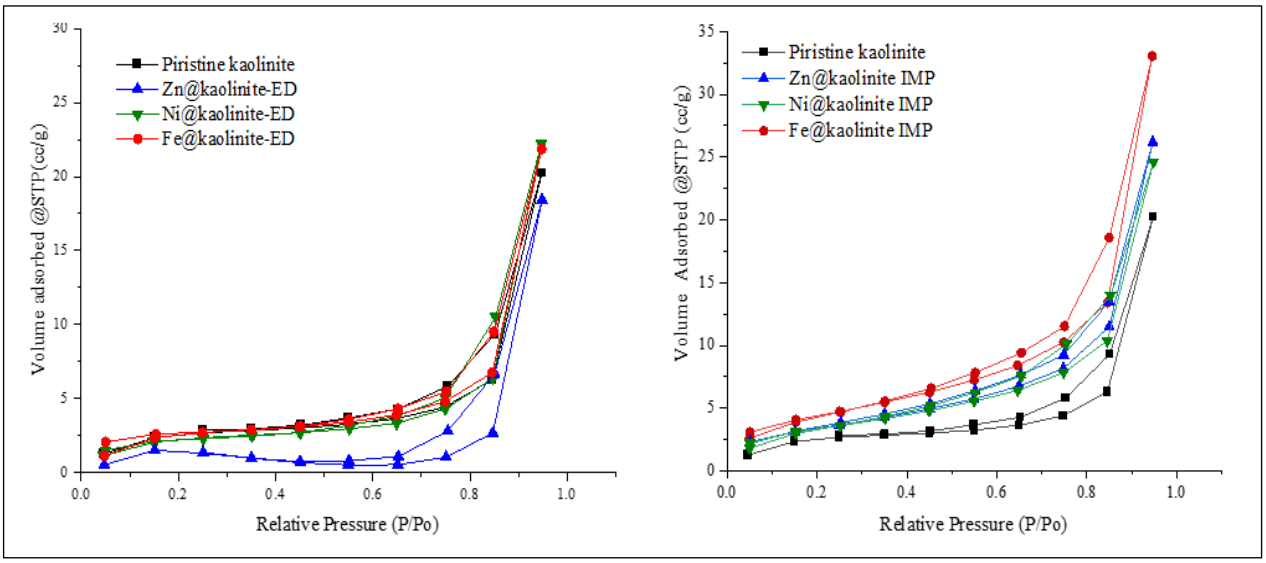

Figure 4 Adsorption and desorption isotherm profiles of pristine kaolinite and TMs@kaolinite photocatalyst by electro-deionization (ED) and impregnation (IMP) methods.

Textural analysis of kaolinite and TMs@kaolinite shows that the surface area of pristine kaolinite increases in the presence of metal (Table 1). The surface area of the TMs@kaolinite IMP tends to be larger than that of TMs@kaolinite ED. A wider surface area promises more active sites for both adsorption and photodegradation. Meanwhile, kaolin's surface area decreased significantly after adding Ni and Zn metals using the ED method. The decrease in catalyst surface area is thought to be caused by the coagulation of Ni and Zn metals on the surface of the Kaolin catalyst, thereby closing the pores of the Kaolin and reducing the surface area of contact between the catalyst's active site and the reactants.

The IMP method produced a catalyst with a smaller average pore radius than the ED method. The average pore radius reduction indicated that some metal particles entered the pores of the kaolinite, so the metal particles blocked the pores. The pristine kaolinite and TMs@kaolinite samples had an average pore size of more than 60 Å, thus, they were classified in the mesoporous region. The Fe@kaolinite IMP has the highest surface area (15.867 m^2/g), meanwile the Zn@kaolinite IMP

has the 2nd large of surface area (12.512 m^2/g). Adding the TMs in the kaolinite has little impact in the increasing of surface area.

Table 1 Comparison the Specific Surface Area, Total Pore Volume, and Average Pore Radius of Catalyst.

Sample	Specific Surface Area (m^2/g)	Total Volume Pore ($x10^{-2}$ cc/g)	Average Pore Radius (Å)
Piristine kaolinite	8.334	3.138	73
Fe@kaolinite ED	8.989	3.389	75
Ni@kaolinite ED	7.615	3.448	91
Zn@kaolinite ED	2.948	2.855	194
Fe@kaolinite IMP	15.867	5.122	65
Ni@kaolinite IMP	12.174	3.815	63
Zn@kaolinite IMP	12.512	4.059	65

3.5. The Photocatalytic Activity

Without a catalyst, the maximum degradation efficiency of methylene blue (MB) reached 22% after one hour of irradiation. The dye degrades even without a catalyst because the chromophore group absorbs photons. The absorbed energy breaks the bonds in the chromophore region of the dye, breaking it down into smaller molecules, which then break down further into simple compounds (Groeneveld *et al.*, 2023). The catalyst sample has a higher efficiency of MB degradation because the metal is a semiconductor, while kaolinite is not. Therefore, the TMs@kaolinite catalyst absorbs light more efficiently.

3.6. The effects of time in photodegradation of MB

Four key elements are required for catalytic photodegradation: a light energy source (photons), a specific compound to be degraded, oxygen as an oxidant, and a photocatalyst. Xenon lamps and sunlight are known to have visible light spectra. The dye model used is methylene blue in aqueous media as the target compound to be degraded. At the same time, air, as a source of oxygen, is an electron acceptor and a photocatalyst made of TMs@kaolinite.

Photodegradation of MB using a TMs@kaolinite photocatalyst was carried out in a controlled process. Stirring was carried out during irradiation to ensure uniformity in the photodegradation reaction and even dispersion of the TMS@kaolinite photocatalyst in methylene blue. Irradiation was carried out several times to study the photocatalytic activity as a function of time (Figure 5). The decrease in methylene blue concentration due to adsorption events that may accompany the photodegradation reaction was also measured as a correction factor for the photocatalytic properties of TMs@kaolinite. Based on the research results, it can be predicted whether methylene blue is only adsorbed or undergoes adsorption and degradation processes simultaneously facilitated by the TMs@kaolinite photocatalyst.

After an hour of exposure, there are no persent MB photodegradation without a catalyst. The dye degrades even without a catalyst because the chromophore group absorbs photons. The absorbed energy breaks the bonds in the chromophore region of the dye, breaking it down into smaller molecules, which then break down further into simple compounds (Groeneveld *et al.*, 2023). The catalyst sample has a higher efficiency of dye degradation because of the metal is a semiconductor, while kaolinite is not. Adding metal to kaolinite showed an increase in the efficiency of photodegradation of MB compared to kaolinite without metal. These results indicate that the photocatalytic activity of MB degradation is effectively increased in the presence of metals. Therefore, the TMs@kaolinite catalyst absorbs light more efficiently. The highest degradation efficiency was achieved using Zn@kaolinite. The degradation efficiency for MB reached 92% after exposure for 60 minutes under natural sunlight. The photodegradation efficiency in this research is higher than previous research, which used a GMC-Fe (Graphitic mesoporous carbon) catalyst under UV light (Ulfa *et al.*, 2023).

Similar studies related the photocatalytic degradation of MB using TiO_2 (Zulmajdi *et al.*, 2019; Suhaimi *et al.*, 2022), kaolin-titania (Kamaluddin *et al.*, 2021) and samarium complexes with 2,6-Naphtalenedicarboxylate ligand (Wulandari, Zulys and Kusrini, 2019)). On the other hand, removal

of MB from aqueous solution using pectin-alginate-titania composite microparticles has been reported by Zamri and her friends (Zamri *et al.*, 2021). Similar study for removal of MB using durian rind has also evaluated by Asbollah and coworkers (Asbollah *et al.*, 2021). According to the previously reported that different forms of catalysts/composites have also different phenomena and mechanisms for photodegradation of MB.

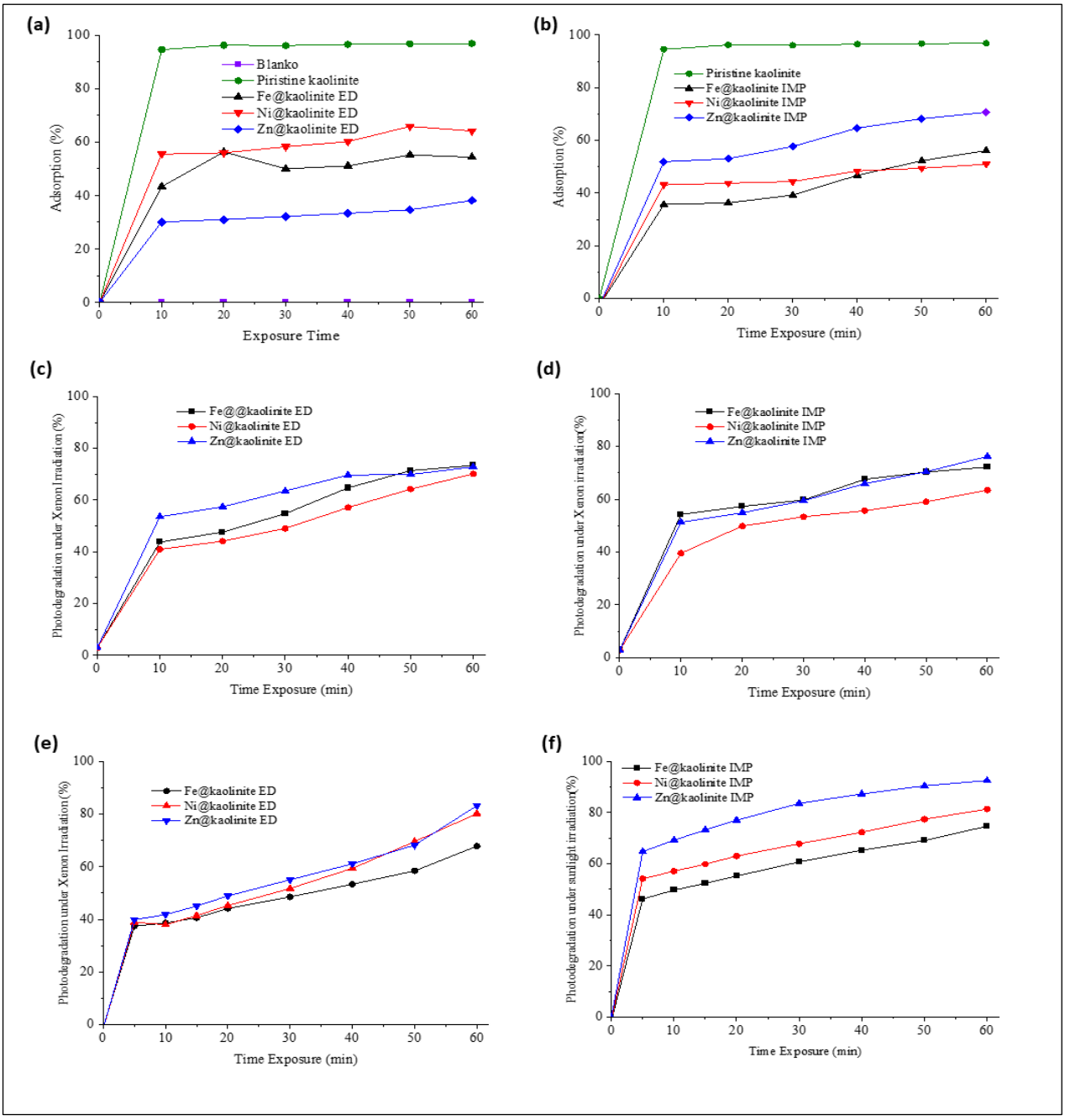

Figure 5 The impact of exposure duration on the adsorption and photodegradation efficiency of MB.

It is interesting to note that the TMs have important role in the performance of the TMs-kaolinite catalysts for photodegradation of MB. We found that the Zn-Kaolinite IMP catalyst is the most excellent photocatalytic activity is with efficiency photodegradation of 92% during 90 minutes of irradiation, even it only has the 2nd large surface area (12.512 m^2/g). Meanwhile, for the rest of TMs including Fe and Ni have photodegradation efficiencies are less than those the Zn modifier (See Figure 5).

3.7. The Adsorption Kinetics

In this study, data analysis steps were carried out systematically better to understand MB absorption kinetics (Figure 6). The first step was to convert the liquid concentration data into the amount of MB absorbed, expressed in qt. These raw data were then plotted in a graph of qt against time (t) to visualize the absorption pattern. Furthermore, data fitting was performed using the asymptotic exponential equation. This equation is used to represent the raw data to facilitate further analysis. The asymptotic exponential equation can calculate a time of less than 10 minutes. In addition, this equation also allows the determination of the amount of MB absorbed at equilibrium conditions (qe), which is an important parameter in the adsorption kinetic analysis.

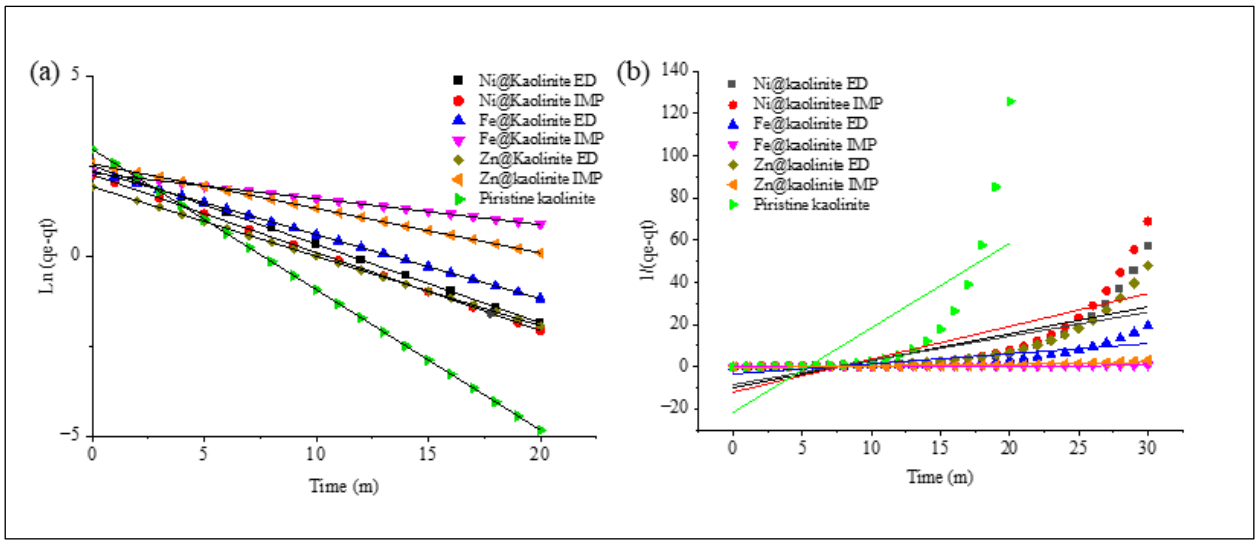

Figure 6 The adsorption kinetics data of MB fitted with (a) pseudo-first order kinetic model and (b) pseudo-second order kinetic model.

The adsorption kinetics data of MB were evaluated using the pseudo-first order and pseudo-second order kinetic models (See Table 2). In this case, the asymptotic exponential equation produces data points (qt, t), which are then processed to obtain qe and qt values. This approach provides a strong basis for quantitatively analyzing the kinetic mechanism of MB removal. This study found that the MB removal of pristine kaolinite and TMs@kaolinite follow pseudo-first-order kinetics with an R^2-value approaching 1.

Table 2 Parameter of adsorption kinetics, where * = multiple (x).

Sample	Pseudo first order equation			Pseudo second order equation	
	Ln (qe-qt) = -kt + ln qe	**R^2**	**k (min^{-1})**	**1/(qe-qt) = k*t + 1/qe**	**R^2**
Piristine kaolinite	Ln(qe-qt)=-0.38976*t+2.96034	1	0.39	1/(qe-qt) = 187.26*t-1226.5	0.616
Ni@kaolinite ED	Ln(qe-qt)=-0.21812*t+2.5046	1	0.218	1/(qe-qt) = 68*t - 864.9	0.510
Ni@kaolinite IMP	Ln(qe-qt)=-0.21625*t+2.25424	1	0.216	1/(qe-qt) = 79.7*t -1012.2	0.512
Fe@kaolinite ED	Ln(qe-qt)=-0.17799*t+2.37235	1	0.18	1/(qe-qt) = 10.79*t-132.78	0.554
Fe@kaolinite IMP	Ln(qe-qt)=-0.07114*t+2.29386	1	0.071	1/(qe-qt) = 0.06*t-0.44	0.814
Zn@kaolinite ED	Ln(qe-qt)=-0.19308*t+1.9204	1	0.19	1/(qe-qt) = 35.563*t-443.983	0.535
Zn@kaolinite IMP	Ln(qe-qt)=-0.12375*t+2.55671	1	0.124	1/(qe-qt) = 0.6361*t-7.05	0.653

This study is comparable with the Lagergren pseudo-first order result that reported by Asbollah and collegues with the R value of 0.997 (Asbollah *et al.*, 2021). Meanwhile, pristine kaolinite has the highest MB removal rate constant compared to TMs@kaolinite. It is noted that the MB removal of pristine kaolinite is the fastest compared to TMs@kaolinite (see Table 2). The study's findings indicated that the kinetic parameters of transition metals are not significantly influenced by their periodic characteristics.

4. Conclusions

The photocatalytic activity of pristine kaolinite and its composites (TMs@kaolinite) to degrade methylene blue (MB) under sunlight or xenon irradiation has been investigated. In this study, TMs@kaolinite photocatalyst was successfully prepared using electro-deionization (ED) and impregnation (IMP) methods to form metal oxides on the kaolin surface. The kaolinite only shows the removal of MB without a degradation process with an adsorption efficiency of 98%. The presence of transition metals (TMs) in TMs-kaolinite catalysts has an important role in the performance of photocatalysts. The Zn@kaolinite IMP was the most effective catalyst in the photodegradation process of azo dyes under sunlight irradiation, with an efficiency of 92%. All of the adsorption kinetics adhered to the pseudo-first-order model. Furthermore, it was discovered that sunlight outperforms xenon lamps for MB photodegradation. In future work, the different TMs and preparation methods for photocatalyst can be further evaluated to obtain the optimum for degradation of azo dye and useful for practical in industries and/or mitigation of climate change and environmentally friendly.

Acknowledgements

The authors are grateful to the Legal Entity State Funding Assistance (BPPTNBH) under the Indonesian Collaboration Research Program (RKI) Scheme C [Decision Letter No. 767/UN27/HK/2023 and Contract No. 590.1/UN27.22/HK.07.00/2023].

Author Contributions

KDN – conceptualization, supervision and analysis; IFN - Analysis, writing & review; DYP – Experiment & Investigation; SJS – Review; EK – Analysis, writing & review; AU- Editing & review: LDW-Review

Conflict of Interest

The authors declare no conflicts of interest.

Supplementary Materials

References

Asbollah, M. Ashrul, Abdul Hanif Mahadi, Eny Kusrini, and Anwar Usman. 2021. "Synergistic Effect in Concurrent Removal of Toxic Methylene Blue and Acid Red-1 Dyes from Aqueous Solution by Durian Rind: Kinetics, Isotherm, Thermodynamics, and Mechanism." *International Journal of Phytoremediation* 23 (13): 1432–43. https://doi.org/10.1080/15226514.2021.1901851.

Asmare, Zinabu Gashaw, Belete Asefa Aragaw, Minaleshewa Atlabachew, and Tessera Alemneh Wubieneh. 2022. "Kaolin-Supported Silver Nanoparticles as an Effective Catalyst for the Removal of Methylene Blue Dye from Aqueous Solutions." *ACS Omega*, January. https://doi.org/10.1021/acsomega.2c05265.

Aviantara, Dwindrata Basuki, Fuzi Suciati, Gunawan Hadiko, Nastiti Siswi Indrasti, and Mohamad Yani. 2024. "Microwave-Assisted Impregnation of Zinc Metal Ions on Surface of Quenched Pulverized Shrimp Shell Waste." *International Journal of Technology* 15 (6): 1946–58. https://doi.org/10.14716/ijtech.v15i6.6170.

Balarabe, Bachir Yaou, Sagar Bowmik, Avijit Ghosh, and Prasenjit Maity. 2022. "Photocatalytic Dye Degradation by Magnetic XFe2O3 (X: Co, Zn, Cr, Sr, Ni, Cu, Ba, Bi, and Mn) Nanocomposites under Visible Light: A Cost Efficiency Comparison." *Journal of Magnetism and Magnetic Materials* 562 (November): 169823. https://doi.org/10.1016/J.JMMM.2022.169823.

Beddiaf, Samiha, Smail Chihi, and Youcef Leghrieb. 2015. "The Determination of Some Crystallographic Parameters of Quartz, in the Sand Dunes of Ouargla, Algeria." *Journal of African Earth Sciences* 106 (June): 129–33. https://doi.org/10.1016/J.JAFREARSCI.2015.03.014.

Cao, Zhou, Qizhao Wang, and Hongfei Cheng. 2021. "Recent Advances in Kaolinite-Based Material for Photocatalysts." *Chinese Chemical Letters* 32 (9): 2617–28. https://doi.org/10.1016/j.cclet.2021.01.009.

Chen, Meijuan, Tongxi Yang, Jichang Han, Yang Zhang, Liyun Zhao, Jinghan Zhao, Rong Li, Yu Huang, Zhaolin Gu, and Jixian Wu. 2023. "The Application of Mineral Kaolinite for Environment Decontamination: A Review." *Catalysts* 13 (1): 123. https://doi.org/10.3390/catal13010123.

Darmadi, Mirna Rahmah Lubis, Munadiya Masrura, Aziz Syahfatra, and Mahidin. 2023. "Clay and Zeolite-Clay Based Monoliths as Adsorbents for the Hg(II) Removal from the Aqueous Solutions." *International Journal of Technology* 14 (1): 129–41. https://doi.org/10.14716/ijtech.v14i1.5134.

Groeneveld, Iris, Maria Kanelli, Freek Ariese, and Maarten R. van Bommel. 2023. "Parameters That Affect the Photodegradation of Dyes and Pigments in Solution and on Substrate – An Overview." *Dyes and Pigments*. Elsevier. https://doi.org/10.1016/j.dyepig.2022.110999.

Hakimi, Bahareh, Mohammad Ghorbanpour, and Atabak Feizi. 2018. "ZnO/Bentonite Nanocomposites Prepared with Solid-State Ion Exchange as Photocatalysts." *Journal of Ultrafine Grained and Nanostructured Materials* 51 (2): 139–46. https://doi.org/10.22059/JUFGNSM.2018.02.05.

Hamrayev, Hemra, and Kamyar Shameli. 2022. "Synthesis and Characterization of Ionically Cross-Linked Chitosan Nanoparticles." *Journal of Research in Nanoscience and Nanotechnology* 7 (1): 7–13. https://doi.org/10.37934/JRNN.7.1.713.

Hariyanto, B., D. A.P. Wardani, N. Kurniawati, N. P. Har, N. Darmawan, and Irzaman. 2021. "X-Ray Peak Profile Analysis of Silica by Williamson–Hall and Size-Strain Plot Methods." *Journal of Physics: Conference Series* 2019 (1). https://doi.org/10.1088/1742-6596/2019/1/012106.

Heriyanto, Heri, Oki Muraza, Galal A. Nasser, Mohammed Ahmed Sanhoob, Idris A. Bakare, Budhijanto, Rochmadi, Karna Wijaya, and Arief Budiman. 2023. "Improvement of Catalyst Activity in Methanol-to-Olefin Conversion via Metal (Sr/La) Impregnation over ZSM-5 Catalyst." *International Journal of Technology* 14 (1): 142–51. https://doi.org/10.14716/ijtech.v14i1.4884.

Holmberg, Brett A., Huanting Wang, and Yushan Yan. 2004. "High Silica Zeolite Y Nanocrystals by Dealumination and Direct Synthesis." *Microporous and Mesoporous Materials* 74 (1–3): 189–98. https://doi.org/10.1016/j.micromeso.2004.06.018.

Ivanić, Maja, Neda Vdović, Sandra de Brito Barreto, Vladimir Bermanec, and Ivan Sondi. 2015. "Mineralogy, Surface Properties and Electrokinetic Behaviour of Kaolin Clays Derived from Naturally Occurring Pegmatite and Granite Deposits." *Geologia Croatica* 68 (2): 139–45. https://doi.org/10.4154/gc.2015.09.

Janíková, Barbora, Jonáš Tokarský, Kateřina Mamulová Kutláková, Martin Kormunda, and Lucie Neuwirthová. 2017. "Photoactive and Non-Hazardous Kaolin/ZnO Composites Prepared by Calcination of Sodium Zinc Carbonate." *Applied Clay Science* 143 (March): 345–53. https://doi.org/10.1016/j.clay.2017.04.003.

Kamaluddin, Muhamad Rafiq, Nur Izzah Iwanina Zamri, Eny Kusrini, Wuwuh Wijang Prihandini, Abdul Hanif Mahadi, and Anwar Usman. 2021. "Photocatalytic Activity of Kaolin–Titania Composites to Degrade Methylene Blue under UV Light Irradiation; Kinetics, Mechanism and Thermodynamics." *Reaction Kinetics, Mechanisms and Catalysis* 133 (1): 517–29. https://doi.org/10.1007/s11144-021-01986-x.

Kusrini, Eny, Abi Rifqi Rafdi, Anwar Usman, Lee D. Wilson, Volkan Degirmenci, Mohd Aidil Adhha Abdullah, and Nofrijon Sofyan. 2024. "Performance Comparison of Heterogeneous Catalysts Based on Natural Bangka Kaolin for Biodiesel Production by Acid and Base Activation Processes." *International Journal of Technology* 15 (6): 1994–2008. https://doi.org/10.14716/ijtech.v15i6.7023.

Li, Chunquan, Xiongbo Dong, Ningyuan Zhu, Xiangwei Zhang, Shanshan Yang, Zhiming Sun, Yangyu Liu, Shuilin Zheng, and Dionysios D. Dionysiou. 2020. "Rational Design of Efficient Visible-Light Driven Photocatalyst through 0D/2D Structural Assembly: Natural Kaolinite Supported Monodispersed TiO2 with Carbon Regulation." *Chemical Engineering Journal* 396 (April): 125311. https://doi.org/10.1016/j.cej.2020.125311.

Li, Tong, Ke Xiao, Bo Yang, Guilong Peng, Fenglei Liu, Liyan Tao, Siyuan Chen, Haoran Wei, Gang Yu, and Shubo Deng. 2019. "Recovery of Ni(II) from Real Electroplating Wastewater Using Fixed-Bed Resin Adsorption and Subsequent Electrodeposition." *Frontiers of Environmental Science and Engineering* 13 (6): 1–12. https://doi.org/10.1007/S11783-019-1175-7/METRICS.

Maged, Ali, Ismael Sayed Ismael, Sherif Kharbish, Binoy Sarkar, Sirpa Peräniemi, and Amit Bhatnagar. 2020. "Enhanced Interlayer Trapping of Pb(II) Ions within Kaolinite Layers: Intercalation, Characterization, and Sorption Studies." *Environmental Science and Pollution Research* 27 (2): 1870–87. https://doi.org/10.1007/s11356-019-06845-w.

Mamulová Kutláková, Kateřina, Jonáš Tokarský, and Pavlína Peikertová. 2015. "Functional and Eco-Friendly Nanocomposite Kaolinite/ZnO with High Photocatalytic Activity." *Applied Catalysis B: Environmental* 162 (January): 392–400. https://doi.org/10.1016/J.APCATB.2014.07.018.

Mousavi, Mitra, Aziz Habibi-Yangjeh, and Masoud Abitorabi. 2016. "Fabrication of Novel Magnetically Separable Nanocomposites Using Graphitic Carbon Nitride, Silver Phosphate and Silver Chloride and Their Applications in Photocatalytic Removal of Different Pollutants Using Visible-Light Irradiation." *Journal of Colloid and Interface Science* 480 (October): 218–31. https://doi.org/10.1016/J.JCIS.2016.07.021.

Mustapha, S., J. O. Tijani, M. M. Ndamitso, S. A. Abdulkareem, D. T. Shuaib, A. K. Mohammed, A. Sumaila, and & A Sumaila. 2020. "The Role of Kaolin and Kaolin/Zno Nanoadsorbents in Adsorption Studies for Tannery Wastewater Treatment." *Scientific Reports 2020 10:1* 10 (1). https://doi.org/10.1038/s41598-020-69808-z.

Nugrahaningtyas, Khoirina Dwi, Eddy Heraldy, Rachmadani, Yuniawan Hidayat, Indriana Kartini, Ferdinand Tri Aji Pamungkas, Aji Gusti, Rachmadani, Yuniawan Hidayat, and Indriana Kartini. 2021. "Effect of Synthesis and Activation Methods on the Character of CoMo/Ultrastable Y-Zeolite Catalysts." *Open Chemistry* 19 (1): 745–54. https://doi.org/10.1515/chem-2021-0064.

Nugrahaningtyas, Khoirina Dwi, Mitha Fitria Kurniawati, Abu Masykur, and Nisriina 'Abidah Quratul'aini. 2022. "Periodic Trends in the Character of First-Row Transition Metals-Based Catalysts Embedded on Mordenite." *Moroccan Journal of Chemistry* 10 (3): 375–86. https://doi.org/10.48317/IMIST.PRSM/morjchem-v10i3.30900.

Nugrahaningtyas, Khoirina Dwi, Eny Kusrini, Salwa Salsabila, Dina Fitriana, Anwar Usman, Triana Kusumaningsih, and Sri Juari Santoso. 2025. "Synthesis of Transition Metal-Nanochitosan Composites Using Ni, Cu, Zn, and Ag Metal Ions and Applications as Antibacterial Agents." *International Journal of Technology* 16 (1): 207–20. https://doi.org/10.14716/ijtech.v16i1.6969.

Pal, Sandhya, Savita Dixit, and Sunder Lal. 2016. "Synthesis and Characterization of Cation Exchange PVA-g-PAA/PBI Sulfone Membrane for the Electrolysis of Sodium Chloride." *Journal of Membrane Science and Research* 2 (3): 147–54. https://doi.org/10.22079/JMSR.2016.20313.

Ramadji, Christian, Adamah Messan, Seick Omar Sore, Elodie Prud'homme, and Philbert Nshimiyimana. 2022. "Microstructural Analysis of the Reactivity Parameters of Calcined Clays." *Sustainability* 14 (4): 2308. https://doi.org/10.3390/su14042308.

Santos, Patrícia B., Hélio F. Dos Santos, and Gustavo F.S. Andrade. 2021. "Photodegradation Mechanism of the RB5 Dye: A Theoretical and Spectroscopic Study." *Journal of Photochemistry and Photobiology A: Chemistry* 416 (March). https://doi.org/10.1016/j.jphotochem.2021.113315.

Seo, Okkyun, Akhil Tayal, Jaemyung Kim, Chulho Song, Yanna Chen, Satoshi Hiroi, Yoshio Katsuya, et al. 2019. "Tuning of Structural, Optical Band Gap, and Electrical Properties of Room-Temperature-Grown Epitaxial Thin Films through the Fe2O3:NiO Ratio." *Scientific Reports 2019 9:1* 9 (1): 1–9. https://doi.org/10.1038/s41598-019-41049-9.

Shao, Godlisten N., Marion Engole, S. M. Imran, Sun Jeong Jeon, and Hee Taik Kim. 2015. "Sol–Gel Synthesis of Photoactive Kaolinite-Titania: Effect of the Preparation Method and Their Photocatalytic Properties." *Applied Surface Science* 331 (March): 98–107. https://doi.org/10.1016/J.APSUSC.2014.12.199.

Sudha, M, and a Saranya. 2014. "Microbial Degradation of Azo Dyes: A Review." *International Journal of Current Microbiology and Applied Sciences* 3 (2): 670–90. http://www.ijcmas.com/vol-3-2/M.Sudha, et al.pdf.

Suhaimi, Nurul Amanina A., Nurulizzatul Ningsheh M. Shahri, Junaidi H. Samat, Eny Kusrini, Jun Wei Lim, Jonathan Hobley, and Anwar Usman. 2022. "Domination of Methylene Blue over Rhodamine B during Simultaneous Photocatalytic Degradation by TiO2 Nanoparticles in an Aqueous Binary Solution under UV Irradiation." *Reaction Kinetics, Mechanisms and Catalysis* 135 (1): 511–27. https://doi.org/10.1007/S11144-021-02098-2/METRICS.

Trindade, Letícia G. da, Marcelo Assis, Josiane C. Souza, Aline B. Trench, Yeison Núñez-de la Rosa, Marcio D. Teodoro, Anderson J. Schwanke, Elson Longo, Fabiana Perrechil, and Anna Rafaela Cavalcante Braga. 2024. "Improving the Photocatalytic Dye Degradation Performance and Bactericidal Properties of Brazilian Amazon Kaolin-Waste by Adding ZnO and Ag3PO4." *Journal of Alloys and Compounds* 971 (January): 172556. https://doi.org/10.1016/j.jallcom.2023.172556.

Trindade, Letícia G Da, Gabriel Yuji Hata, Josiane Carneiro Souza, Mario R S Soares, Edson Roberto Leite, Ernesto C Pereira, Elson Longo, and Tatiana Martelli Mazzo. 2019. "Preparation and Characterization of Hematite Nanoparticles-Decorated Zinc Oxide Particles (ZnO/Fe 2 O 3) as Photoelectrodes for Solar Cell Applications." *Journal of Materials Science* 55. https://doi.org/10.1007/s10853-019-04135-x.

Tsaviv, J. N., I. S. Eneji, R. Shato'Ato, I. Ahemen, P. R. Jubu, and Y. Yusof. 2024. "Photodegradation, Kinetics and Non-Linear Error Functions of Methylene Blue Dye Using SrZrO3 Perovskite Photocatalyst." *Heliyon* 10 (14): e34517. https://doi.org/10.1016/j.heliyon.2024.e34517.

Türkyılmaz, Şenay Şen, Nuray Güy, and Mahmut Özacar. 2017. "Photocatalytic Efficiencies of Ni, Mn, Fe and Ag Doped ZnO Nanostructures Synthesized by Hydrothermal Method: The Synergistic/Antagonistic Effect between ZnO and Metals." *Journal of Photochemistry and Photobiology A: Chemistry* 341 (May): 39–50. https://doi.org/10.1016/J.JPHOTOCHEM.2017.03.027.

Ulfa, Maria, Yuvita Eka Pertiwi, Teguh Endah Saraswati, Hasliza Bahruji, and Holilah Holilah. 2023. "Synthesis of Iron Triad Metals-Modified Graphitic Mesoporous Carbon for Methylene Blue Photodegradation." *South African Journal of Chemical Engineering* 45 (May): 149–61. https://doi.org/10.1016/j.sajce.2023.05.008.

Wang, Jie, Liangjie Fu, Huaming Yang, Xiaochao Zuo, and Di Wu. 2021. "Energetics, Interlayer Molecular Structures, and Hydration Mechanisms of Dimethyl Sulfoxide (DMSO)-Kaolinite Nanoclay Guest-Host Interactions." *Journal of Physical Chemistry Letters* 12 (40): 9973–81. https://doi.org/10.1021/acs.jpclett.1c02729.

Wang, Xiaoxuan, Jinming Jiang, and Weijun Gao. 2022. "Reviewing Textile Wastewater Produced by Industries: Characteristics, Environmental Impacts, and Treatment Strategies." https://doi.org/10.2166/wst.2022.088.

Wongso, Viona, Chew Jing Chen, Abdul Razzaq, Norashikin Ahmad Kamal, and Nonni Soraya Sambudi. 2019. "Hybrid Kaolin/TiO2 Composite: Effect of Urea Addition towards an Efficient Photocatalyst for Dye Abatement under Visible Light Irradiation." *Applied Clay Science* 180 (May): 105158. https://doi.org/10.1016/j.clay.2019.105158.

Wulandari, Dwi Aprillia, Agustino Zulys, and Eny Kusrini. 2019. "Samarium Complexes from 2,6-Naphtalenedicarboxylate: Synthesis, Photocatalytic Properties and Degradation of Methylene Blue." In *IOP Conference Series: Materials Science and Engineering*. Vol. 546. https://doi.org/10.1088/1757-899X/546/4/042050.

Yahaya, Shehu, Suzi Salwah Jikan, Nur Azam Badarulzaman, and Ajiya Dahiru Adamu. 2017. "Chemical Composition and Particle Size Analysis of Kaolin." *Path of Science* 3 (10): 1001–4. https://doi.org/10.22178/pos.27-1.

Zamri, Nur Izzah Iwanina, Siti Lailatul N. Zulmajdi, Nur Zafirah A. Daud, Abdul Hanif Mahadi, Eny Kusrini, and Anwar Usman. 2021. "Insight into the Adsorption Kinetics, Mechanism, and Thermodynamics of Methylene Blue from Aqueous Solution onto Pectin-Alginate-Titania Composite Microparticles." *SN Applied Sciences* 3 (2). https://doi.org/10.1007/s42452-021-04245-9.

Zhang, Yuhan, Xuesong Zhao, Baoyue Shang, Xuesong Wang, Xiulin Wu, and Tingting Li. 2024. "Characterization of Nano-Kaolin and Its Enhancement of the Mechanical and Corrosion Resistance of Epoxy Coatings." *Materials Today Communications* 41 (September). https://doi.org/10.1016/j.mtcomm.2024.110371.

Zulmajdi, Siti Lailatul N., Nur Izzah Iwanina Zamri, Hartini M. Yasin, Eny Kusrini, Jonathan Hobley, and Anwar Usman. 2019. "Comparative Study on the Adsorption, Kinetics, and Thermodynamics of the Photocatalytic Degradation of Six Different Synthetic Dyes on TiO_2 Nanoparticles." *Reaction Kinetics, Mechanisms and Catalysis 2019 129:1* 129 (1): 519–34. https://doi.org/10.1007/S11144-019-01701-X.

Zyoud, Ahed H., Amani Zubi, Samer H. Zyoud, Muath H. Hilal, Shaher Zyoud, Naser Qamhieh, Abdul Razack Hajamohideen, and Hikmat S. Hilal. 2019. "Kaolin-Supported ZnO Nanoparticle Catalysts in Self-Sensitized Tetracycline Photodegradation: Zero-Point Charge and PH Effects." *Applied Clay Science* 182 (September). https://doi.org/10.1016/j.clay.2019.105294.